

Capacity Analysis of UWB Networks in Three-Dimensional Space

Lin X. Cai, Lin Cai, Xuemin (Sherman) Shen, and Jon W. Mark

Abstract: Although asymptotic bounds of wireless network capacity have been heavily pursued, the answers to the following questions are still critical for network planning, protocol and architecture design: Given a three-dimensional (3D) network space with the number of active users randomly located in the space and using the wireless communication technology, what are the expected per-flow throughput, network capacity, and network transport capacity? In addition, how can the protocol parameters be tuned to enhance network performance? In this paper, we focus on the ultra wideband (UWB) based wireless personal area networks (WPANs) and provide answers to these questions, considering the salient features of UWB communications, i.e., low transmission/interference power level, accurate ranging capability, etc. Specifically, we demonstrate how to explore the spatial multiplexing gain of UWB networks by allowing appropriate concurrent transmissions. Given 3D space and the number of active users, we derive the expected number of concurrent transmissions, network capacity and transport capacity of the UWB network. The results reveal the main factors affecting network (transport) capacity, and how to determine the best protocol parameters, e.g., exclusive region size, in order to maximize the capacity. Extensive simulation results are given to validate the analytical results.

Index Terms: Network capacity, three-dimensional (3D) space, ultra wideband (UWB) based wireless personal area networks (WPANs).

I. INTRODUCTION

Ultra wideband (UWB) is an emerging technology to meet the ever-increasing demand for anytime, anywhere wireless services. With high data rate and low transmission power and interference, UWB will enable new multimedia applications that may be beyond what consumers can imagine today [1]. For instance, in broadband hotspots such as Olympic game venues and World Expo centers, all possible multimedia applications requiring high-speed Internet access and/or exchanging information locally can be realized. To facilitate high dense applications in UWB networks, the following issues are very critical for network planning, protocol and architecture design: Given a three-dimensional (3D) space, the number of active users, and the use of UWB communication technologies, what are (i) the expected

number of flows that can transmit concurrently and (ii) the expected per-flow throughput, network throughput capacity, and transport capacity?

The capacity of point-to-point wireless communication over an additive white Gaussian channel was laid out by Claude Shannon in his 1948 seminal paper [2]. With the state-of-the-art channel coding, e.g., turbo code, energy and bandwidth efficiency of practical point-to-point communications is pushing closer to the Shannon limit. Due to the broadcast property of the wireless channel, wireless capacity in a multipoint-to-multipoint *networked* environment is interference limited. How to efficiently deploy the spatial utilization of wireless channel to improve the capacity of wireless networks has been a key challenging issue for several decades. In addition to the time and frequency domains, there is the spatial domain that offers diversity/multiplexing gain. Also the wireless network capacity depends on random network topology. Although asymptotic bounds of wireless network capacity have been heavily pursued, how to fully explore the spatial multiplexing gain of UWB networks and determine the capacity for the networks with random topology are still open issues.

In this paper, we first study how to explore the spatial reuse opportunities of UWB based wireless personal area networks (WPANs), considering the special characteristics of UWB communications. Since UWB has accurate ranging and low transmission/interference power level [3], [4], appropriate scheduling of concurrent transmissions is feasible and favorable, if the transmitters are outside the exclusive regions (ER) of the non-intended receivers. Given a 3D space and the number of active users in the network, we derive the expected number of concurrent transmissions, network capacity and transport capacity of UWB based wireless networks. Here, network capacity is defined as the total throughput (bps) of all flows in the network and network transport capacity is defined as the sum of the products of each flow's throughput and its transceiver distance in the network (bit-m/s). In general, network capacity is the main performance index for single-hop wireless access networks while network transport capacity is for multi-hop wireless networks. The analytical results obtained reveal the main factors that affect network (transport) capacity, which will provide important guidelines for UWB network planning, protocol and architecture design and optimization. For examples, how can the ER size be determined to maximize the network capacity or transport capacity? What is the user density in order to reach the highest expected network (transport) capacity? What are the impacts of different path loss exponents and wireless fading parameters?

The main contributions of the paper are three-fold. First, we re-visit the capacity problem of wireless networks considering the channel characteristics and rate-adaptive feature of UWB

Manuscript received December 19, 2007; approved for publication by Xiaodai Dong, Division II Editor, May 6, 2008.

This work has been supported in part by the Natural Sciences and Engineering Research Council (NSERC) of Canada. The authors would like to thank Mr. Hangguan Shan for his Nakagami channel codes and valuable discussions.

L. X. Cai, X. (Sherman) Shen, and J. W. Mark are with the Centre for Wireless Communications in the Department of Electrical and Computer Engineering, University of Waterloo, Waterloo, ON N2L 3G1, Canada, email: {lcai, xshen, jwmark}@bbcr.uwaterloo.ca.

L. Cai is with the Department of Electrical and Computer Engineering, University of Victoria, email: cai@uvic.ca.

communications. Based on the model, we study how to explore the network capacity and transport capacity of UWB-based WPANs by allowing concurrent transmissions appropriately. Second, we analytically derive the expected capacity of UWB WPANs in 3D space. Extensive simulation results are given to validate the accuracy of the analysis. Finally, the analytical results are used to determine the protocol parameters such as ER size to further improve the network performance. Our approach can also be extended to quantify the capacity of other wireless networks, in general.

The remainder of the paper is organized as follows. Related work is discussed in Section II while the system model is presented in Section III. An analytical framework is developed to investigate the network capacity and transport capacity of UWB based wireless networks in Section IV, followed by numerical results in Section V. Concluding remarks are given in Section VI.

II. RELATED WORK

Capacity bounds of wireless networks have been extensively studied in the literature. In the pioneer work of Gupta and Kumar [5], the asymptotic bounds of network transport capacity have been derived given the node density in an arbitrary or random wireless network. They extended their work to a 3D space in [6] considering all nodes are located in a sphere. Since then, a large number of follow-up papers has appeared. The impact of user mobility on network capacity has been studied in [7], [8]. It was found that node mobility can be exploited to increase the network capacity [7] but excessive mobility contrarily limits the capacity [8]. The capacity of different networks with different traffic patterns, e.g., relay traffic, convergent traffic (in sensor networks), and broadcast traffic, have been investigated in [9]–[12]. The upper and lower bounds of throughput capacity of UWB networks have been derived in [13], [14], considering power constraints of UWB communications and link layer packet loss. Based on the same communication model as that in [5], it was found in [13] that different properties of the physical layer may dramatically alter the network capacity. In contrast with the result in [5] that the capacity per node is a decreasing function of node density, the capacity bounds derived in [13] increase with the node density assuming that the interference is negligible for UWB networks with low transmission power. To the best of our knowledge, most of the previous work studied the capacity region, or the upper/lower bounds on network capacity based on the two transmission models proposed in [5]: The protocol model and the physical model. In the protocol model, the transmission between two nodes X_i and X_j is successful if

$$|X_k - X_j| \geq (1 + \Delta)|X_i - X_j|$$

for every other node X_k simultaneously transmitting over the same subchannel. In other words, to ensure the transmission from X_i to X_j to be successful, there is a guard zone centered at X_j with radius proportional to $|X_i - X_j|$, as shown in Fig. 1 [5]. No other node inside the guard zone should transmit concurrently. In the physical model, a transmission from a node X_i is

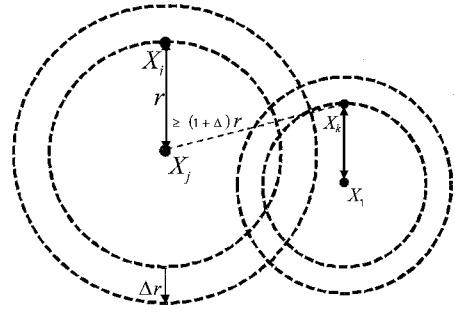


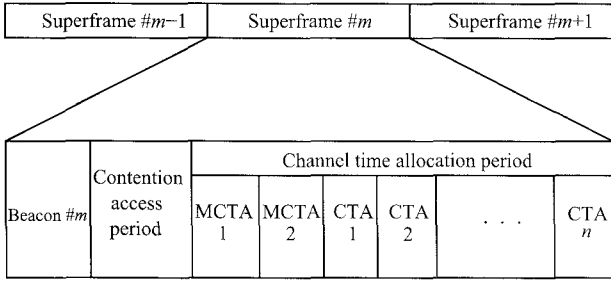
Fig. 1. Protocol model.

successfully received by a node X_j if

$$\frac{P_i}{P_n + \sum_{k \neq i} \frac{P_k}{|X_k - X_j|^\alpha}} \geq \beta$$

where P_i and P_k are the transmission power levels of node X_i and X_k , respectively, P_n is the ambient noise power level, and α is the path loss exponent. This model indicates that the transmission from X_i to X_j can be successful only if the signal to interference and noise ratio (SINR) at the receiver exceeds a certain threshold. If not, the transmission will fail and the flow throughput will be zero. In these two models, the transmission rate is a binary function, which is simple and thus analytically attractive for capacity analysis. However, with the recent advances in wireless technologies, the two models are no longer applicable in some emerging wireless networks. For instance, in UWB communication networks, the sender can adjust the data rate according to the received SINR. Such rate adaptation scheme is also used in other wireless communication systems (e.g., IEEE 802.11, IEEE 802.15.3c). Therefore, even if there is an interferer which is located inside the guard zone specified in the protocol model in [5], the flow throughput may not immediately drop to zero. Moreover, there is no single threshold β (in the physical model in [5]) that decides the transmission rate, which is adaptive according to SINR. To model realistic UWB networks, it is necessary to employ a more general communication model that captures the rate adaptation in the physical layer. In addition, the asymptotic capacity bounds derived in the previous work, especially those for arbitrary networks, may be too loose to be useful in realistic networks where the network topology is random and may change from time to time due to user mobility. Therefore, we are more interested in deriving the expected network capacity or network transport capacity of a random network, and maximizing them by fine tuning the protocol parameters.

On the other hand, existing theoretical studies indicate that to improve the resource utilization, it is optimal to allow concurrent transmissions, as long as all interferers are outside a well-defined ER around the destinations [15]. It is shown in [16]–[18] that ER based resource management can significantly improve the network throughput by exploiting the spatial dimension of the wireless channel. But ER condition obtained in [16] is only a sufficient condition to ensure that concurrent transmission is



MCTA: Management channel time allocations
CTA: Channel time allocations

Fig. 2. Superframe structure defined in IEEE 802.15.3 MAC protocol.

preferable. The optimal ER size to maximize the capacity of grid and hexagon cellular networks are obtained in [17] and [18], respectively. However, realistic networks are usually deployed in a random fashion, and the assumptions of ideal grid or hexagon topologies do not hold in general. To the best of our knowledge, how to control the interference level and optimize the ER size to maximize the network capacity and transport capacity of a network in 3D space is still an open issue.

III. SYSTEM MODEL

A. Network Model

We consider a densely deployed IEEE 802.15.3 based UWB WPAN consisting of N flows, $\{f_i | i \in 1, 2, \dots, N\}$, with the piconet as the basic network element. Devices are randomly and uniformly located in an $l \times l \times h$ space. In each piconet, there is a piconet controller (PNC), which provides the basic timing in the WPAN. Channel time takes the superframe structure, as shown in Fig. 2. Each superframe starts with a beacon period (BP) followed by a short optional contention access period (CAP) and a channel time allocation period (CTAP). The PNC broadcasts network synchronization and control messages during the BP. In the CAP, devices send their transmission requests to the PNC using carrier sense multiple access/collision avoidance (CSMA/CA) in conjunction with a backoff procedure. Based on the successfully received requests, the PNC allocates wireless resources to the devices so they can communicate with each other directly without contentions in the following CTAP. In this paper, we focus on how to appropriately utilize the wireless resources in the CTAP. Our approach is to schedule concurrent transmissions in the CTAP to improve the spatial multiplexing capacity of UWB WPANs.

B. Communication Model

According to the Shannon limit of an AWGN channel, the upper bound of the achievable data rate of node j is

$$R_j = W \log_2 \left(1 + \frac{G_{ij} P_i}{(N_0 W + \sum_{k \in \gamma, k \neq i} C_0 G_{kj} P_k)} \right) \text{ bps}$$

where P_i and P_k are the transmission power levels of the sender i and an interferer k , respectively, G_{ij} is the channel gain between nodes i and j , γ is the set of flows that transmit con-

Table 1. List of notations.

Symbol	Description
R_j	The achievable data rate of node j
W	The signal bandwidth
P_i	The transmission power of sender i
N_0	One-sided power spectral density of AWGN
$d_{j,i}$	The distance between the sender of flow j and the receiver of flow i
d_i	The distance between the sender and receiver of the i th flow
α	The path loss exponent
G_{ij}	The channel gain between nodes i and j
γ	The set of flows that transmit concurrently
C_0	The cross correlation coefficient among concurrent transmissions
K	The average channel gain at the reference distance
S	A random variable denoting the normalized instantaneous channel gain between the transmitter and the receiver
S_i	A random variable denoting the normalized instantaneous channel gain between the i th interferer and the receiver
η	The efficiency of the transceiver
N	The total number of flows in the network
$p(k, n)$	The probability that k from n flows satisfy the concurrent transmission condition
Q	The probability that a sender is outside the ER of a receiver
r	The ER radius
Z	A random variable denoting the transmission distance
Z'	A random variable denoting the effective transmission distance
V_i	A random variable denoting the interference distance (from the i th interferer to a receiver)
G_T	The antenna gain of the transmitter
G_R	The antenna gain of the receiver
I_1	The interference level resulting from an interferer
$E[T_S]$	The expected data rate of a single flow during transmission
$E[Tr_S]$	The expected bit-meter product of a single flow
$E[T]$	The expected network capacity
$E[Tr]$	The expected network transport capacity

currently, C_0 is the cross correlation coefficient among concurrent transmissions, N_0 is the one-sided power spectral density of additive white Gaussian noise (AWGN), and W is the signal bandwidth. The notations used in the paper are listed in Table 1 for easy reference. Due to the low power level of UWB systems, complex power control scheme can only provide marginal throughput gain [15]. Therefore, in our system model, all UWB nodes transmit with the maximum power P .

Wireless media access control (MAC) protocol generally uses exclusive mechanisms to avoid collisions among simultaneous channel accesses. If all flows share the same channel, the cross

correlation coefficient among concurrent transmissions (C_0) equals 1. In contrast, some spread spectrum techniques, either in the time domain (e.g., direct sequence spread spectrum) or in the frequency domain (e.g., frequency-hopping spread spectrum), can also be used to mitigate interference thus allow for more aggressive spatial multiplexing, with $C_0 \ll 1$.

The channel gain is a function of path loss, fading and shadowing. It is modeled as

$$G_{ij} = K S d_{i,j}^{-\alpha} \quad (1)$$

where $d_{i,j}$ is the distance between the sending node i and the receiving node j , α is the path loss exponent, K is the average channel gain at the reference distance, and S captures the fast fading characteristics. S equals the instantaneous channel gain normalized by its time-average value. In general, UWB fast fading characteristics fit the Nakagami distribution [19]. Thus, we evaluate the network performance considering independent Nakagami fading channels between any two nodes in the system model, and study the impact of the Nakagami factors. Notice that the receiver's SINR is subject to the noise and interference from other concurrent transmissions where interference between nodes j and k also depends on the channel gain G_{kj} .

C. Exclusive Region Based Concurrent Transmissions

Let k flows transmit in k time slots and we compare the performance of the following two scheduling schemes: a) Assign each slot to a single flow exclusively in a round-robin time division multiple access (TDMA) fashion; and b) all flows transmit concurrently in all k time slots. Using the first scheme, without interference, the instantaneous throughput of each flow in its assigned slot is higher; using the second concurrent transmission scheme, the instantaneous throughput of each flow is lower due to mutual interference, but each flow can transmit during more time slots.

To investigate when the concurrent transmission scheme is preferable, we compare the achievable per-flow throughputs of the two schemes using the Shannon capacity. The achievable throughput of a flow using the TDMA scheme is smaller than that of the concurrent transmission scheme if the interference to the flow is less than $k - 1$ times the noise level [16]. In other words, we obtain a sufficient condition to ensure that the concurrent transmission scheme is favorable: the interference level from any other concurrently transmitting flows should be less than the noise level, independent of the transceiver distance. Therefore, in a 3D space, we can define an ER for concurrent transmissions. If all $k - 1$ interferers are located outside the ER, the interference at the receiver would be less than $k - 1$ times the background noise level, so concurrent transmissions would be more favorable. With all senders transmitting at the same power level P and using the path loss model in (1), the ER can be a sphere centered at the receiver with radius r , as shown in Fig. 3. In the figure, flows f_1, f_2, f_4 , and f_5 can concurrently transmit since all senders are outside the ERs of other receivers, while flow f_3 conflicts with flow f_2 or flow f_4 and they cannot be transmitted concurrently. With accurate ranging capability of UWB communications, it is feasible and practical to determine whether an interferer is outside the ER of a receiver or not.

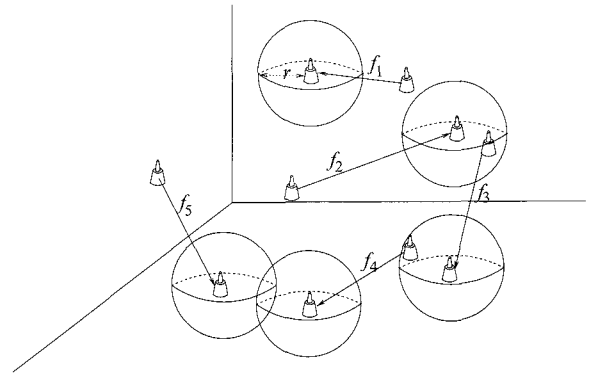


Fig. 3. Exclusive region for concurrent transmissions.

Different from the guard zone specified in the protocol model in [5], the general ER employed in our system model is independent of the transceiver distance, but is related to the interference and noise levels. Based on the concept of the ER, we can efficiently utilize the wireless resources by allowing appropriate concurrent transmissions: If the senders of a number of flows are outside the ERs of all other receivers, they can concurrently transmit to achieve high spatial multiplexing gain. An important objective is to control the interference level and optimize the ER parameter r to maximize the spatial multiplexing gain of a random topology network. In the following, we derive the average number of concurrent transmissions, the throughput of a single flow, and the network capacity, given an ER size. The results can be used to choose the best ER size to maximize the network capacity.

IV. ANALYTICAL MODEL

We consider an IEEE 802.15.3 based UWB WPAN with N flows, $\{f_i | i \in 0, 1, \dots, N\}$. Denote the distance between the sender and receiver of the i th flow by d_i , and the distance between the sender of flow j and the receiver of flow i by $d_{j,i}$. All senders use the same transmission power P .

To explore the spatial reuse of wireless channels, the scheduling scheme allowing appropriate concurrent transmission takes the following procedure. For each time slot to be scheduled, we first randomly select one flow and add it to the set γ for transmission. Then, we check other flows one by one in a random sequence and add another flow to the set γ if and only if this flow does not conflict with all flows in the set γ , i.e., all the senders are outside the ER of the receivers including the new flow. This procedure continues until all N flows are examined.

A. Number of Concurrent Transmissions

Without loss of generality, the flows being checked by the scheduling algorithm are labeled flow $1, 2, \dots, N$. Given the ER radius r , let $p(k, n)$ denote the probability that k flows satisfy the concurrent transmission condition, after checking the first $n (\leq N)$ flows one by one. The first flow f_1 is always scheduled for transmission and added to the set γ , and we have $p(1, 1) = 1$. The second flow f_2 will be added to the set γ if it does not conflict with f_1 . Let the random variable Z be the distance between two devices randomly located in an $l \times l \times h$ 3D space. Denote

Q the probability of another sender outside the ER of a receiver, i.e., the distance between the sender (of flow j) and the receiver (of flow i) is larger than r ,

$$Q = \Pr(d_{j,i} \geq r) = \int_r^{\sqrt{2l^2+h^2}} f_Z(z) dz \quad (2)$$

where $f_Z(z)$ is the probability density function (pdf) of Z , which is derived in the APPENDIX. The probability that a flow does not conflict with another flow is Q^2 , because the sender of each flow should be outside the ER of the other flow's receiver. Accordingly, the probability that a flow conflicts with another flow is $1 - Q^2$. Therefore, we have $p(2, 2) = Q^2$ and $p(1, 2) = 1 - Q^2$. When we check the first n flows, there are k flows in the set γ if a) there are $k - 1$ flows in γ for the first $n - 1$ flows, and the n th flow does not conflict with the $k - 1$ flows in γ ; or b) there are k flows in γ after we check the first $n - 1$ flows, and the n th flow conflicts with at least one of the k flows. We have

$$p(k, n) = p(k - 1, n - 1)Q^{2(k-1)} + p(k, n - 1)(1 - Q^{2k}) \quad \text{for } k < n. \quad (3)$$

If only the first flow can be added to γ , implying that the following $n - 1$ flows do not satisfy the concurrent transmission condition, we have

$$p(1, n) = (1 - Q^2)^{n-1}. \quad (4)$$

Another extreme case is that all n flows can transmit concurrently, which means that none of the flows conflicts with the remaining $n - 1$ flows. Thus,

$$p(n, n) = Q^{(n-1)n}. \quad (5)$$

Given $p(1, 1)$, $p(1, 2)$, and $p(2, 2)$, we can iteratively obtain $p(k, N)$ as a function of r for $1 \leq k \leq N$. The expected number of concurrent transmissions is thus given by

$$E[N] = \sum_{k=1}^N kp(k, N). \quad (6)$$

B. Network Capacity and Transport Capacity

Given the transmission distance z' , transmission power P , and the channel gain s between the transmitter and the receiver, the received signal power, P_R , is given by

$$P_R = KG_T G_R z'^{-\alpha} s P \quad (7)$$

where K is a constant, G_T and G_R are the antenna gains of the transmitter and receiver, respectively. Accordingly, the achievable data rate of the flow is calculated as

$$R = \eta W \log_2 \left(1 + \frac{KG_T G_R z'^{-\alpha} s P}{N_0 W + I} \right) \quad (8)$$

where η is a constant coefficient related to the efficiency of the transceiver design. Since the UWB fast fading characteristics

follow the Nakagami distribution [19], the pdf of the Nakagami channel gain is given by

$$f_S(s) = \left(\frac{m}{\omega} \right)^m \frac{s^{m-1}}{\Gamma(m)} e^{-\frac{ms}{\omega}} \quad (9)$$

where m is the Nakagami parameter denoting the channel fading conditions and ω is the average received power. Notice that (8) does not apply when $z' \rightarrow 0$, and the achievable data rate is actually bounded in realistic communication systems. We assume that the maximum data rate is achieved when the transmission distance is not larger than the reference distance d_{\min} , $z' \leq d_{\min}$. Let the random variable Z' denote the effective transmission distance, which can be represented as a truncated random variable over $[d_{\min}, \sqrt{2l^2 + h^2}]$. The probability density function of Z' is

$$f_{Z'}(z') = \begin{cases} \delta(z' - d_{\min}) \int_0^{d_{\min}} f_Z(z) dz & \text{for } z' = d_{\min} \\ f_Z(z') & \text{for } d_{\min} < z' \leq \sqrt{2l^2 + h^2}. \end{cases} \quad (10)$$

Denote the interference distance and the gain of the channel between the i th interferer to a receiver as random variables V_i over $[r, \sqrt{2l^2 + h^2}]$ and S_i , respectively. The pdf of V_i is given by

$$f_{V_i}(v) = \frac{f_Z(v)}{\int_r^{\sqrt{2l^2+h^2}} f_Z(z) dz}. \quad (11)$$

The UWB channel between the interferer and the receiver also uses Nakagami fading model and the pdf of random variable (RV) S_i is the same as (9).

Given the interference distance v and the channel fading factor s_i , the interference from a single interferer is

$$I_1 = KC_0 G_T G_R v^{-\alpha} s_i P. \quad (12)$$

Given that there are k concurrently transmitting flows, each flow has $k - 1$ interferers. Since the received signal strength and the interference strength are independent RVs, the received SINR of a single flow can be obtained as

$$\begin{aligned} \text{SINR}|k &= KG_T G_R z'^{-\alpha} s P / [N_0 W + \sum_{i=1}^{k-1} I_i] \\ &\approx KG_T G_R P s z'^{-\alpha} / [N_0 W + (k - 1) I_1]. \end{aligned} \quad (13)$$

Accordingly, the average transmission rate and the bit-meter product of a single flow under $k - 1$ interferers are given by

$$\begin{aligned} E[T_S|k] &= \eta W E[\log_2(1 + \text{SINR}|k)] \\ &\approx \iiint \iiint \eta W \log_2 \left(1 + \frac{KG_T G_R z'^{-\alpha} s P}{N_0 W + (k - 1) KC_0 G_T G_R P v_i^{-\alpha} s_i} \right) \\ &\quad \cdot f_{V_i}(v_i) f_{S_i}(s_i) f_S(s) f_{Z'}(z') dv_i ds_i ds dz' \end{aligned} \quad (14)$$

and

$$\begin{aligned} E[Tr_S|k] &= \iiint \iiint z' \eta W \log_2 \left(1 + \frac{KG_T G_R z'^{-\alpha} s P}{N_0 W + (k - 1) KC_0 G_T G_R P v_i^{-\alpha} s_i} \right) \\ &\quad \cdot f_{V_i}(v_i) f_{S_i}(s_i) f_S(s) f_{Z'}(z') dv_i ds_i ds dz'. \end{aligned} \quad (15)$$

We then remove the condition of $k - 1$ interferers to obtain the average single flow throughput $E[T_S]$ and bit-meter product $E[Tr_S]$ when it is scheduled for transmission as

$$E[T_S] = \sum_{k=1}^N E[T_S|k]p(k, N) \quad (16)$$

and

$$E[Tr_S] = \sum_{k=1}^N E[Tr_S|k]p(k, N) \quad (17)$$

where $p(k, N)$ is obtained in Section IV-A.

The capacity and transport capacity of the network are the sum of the throughput and bit-meter products of all flows concurrently transmitting, which are obtained as

$$E[T] = \sum_{k=1}^N kE[T_S|k]p(k, N) \quad (18)$$

and

$$E[Tr] = \sum_{k=1}^N kE[Tr_S|k]p(k, N). \quad (19)$$

Given the system parameters such as α , C_0 , P , etc., $E[T]$ and $E[Tr]$ can be obtained as a function of r . Consequently, we can obtain the best value of r to maximize network capacity and transport capacity.

V. NUMERICAL RESULTS

We use Maple 10 to calculate the analytical results and validate them through extensive simulations. The experimental network is set up in a $10 \text{ m} \times 10 \text{ m} \times 2 \text{ m}$ space and flows with distinctive senders and receivers are randomly deployed in the space. We consider the use of omni-directional antenna in a UWB network, and the antenna gains are $G_T = G_R = 1$. The parameters used in the analysis and simulations are listed in Table 2. All flows use the maximum transmission power of 0.037 mW. The background noise level is $N_0 = -117 \text{ dBm/MHz}$ over a 500 MHz signal bandwidth. The path loss exponent is 4 if not otherwise specified. The reference distance is set as $d_{\min} = 1 \text{ m}$ and the path loss at d_{\min} is 43.9 dB. We set the transceiver efficiency $\eta = 0.189$ so the expected achievable data rate at 1 m is $R = \eta W \log_2(1 + \text{SINR}) = 1 \text{ Gbps}$. The cross correlation coefficient C_0 takes the values of 0.1 or 1. In the simulations, the scheduler assigns time slots to flows that can be transmitted concurrently using the random selection algorithm introduced in Section IV. We also use the UWB channel proposed in [19] to study the impact of channel fading on the network performance. Independent Nakagami fading channels with $\omega = 1$ and $m = 1 \sim 6$ are applied between any two nodes. We repeat each simulation 500 times with different random seeds and calculate the average values.

A. Number of Concurrent Transmissions

We study the the expected number of concurrent transmissions, $E[N]$, under various ER sizes and network densities. As

Table 2. Simulation parameters.

Signal bandwidth (W)	500 MHz
Transmission power (P)	0.037 mW
Noise power density (N_0)	-117 dBm/MHz
Path loss exponent (α)	4
Reference distance (d_{\min})	1 m
Path loss at d_{\min} (PL_0)	43.9 dB
Cross correlation (C_0)	0.1~1
Nakagami factor (m)	1~6
Transceiver efficiency (η)	0.189

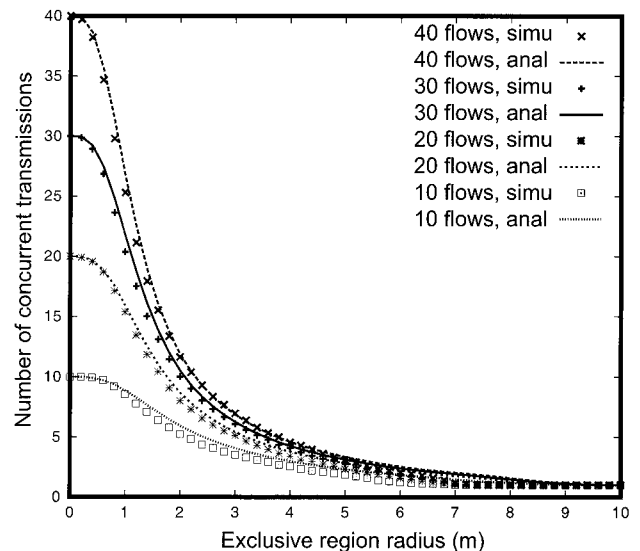


Fig. 4. Expected number of concurrent transmissions vs. ER radius.

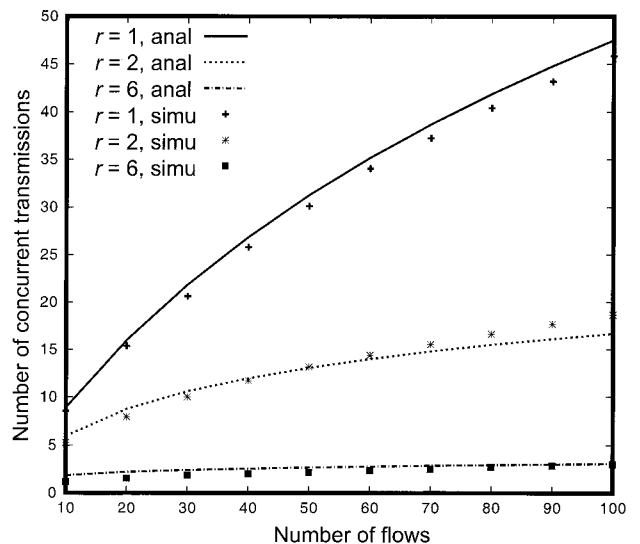


Fig. 5. Expected number of concurrent transmissions vs. number of flows.

shown in Fig. 4, the expected number of concurrent transmissions decreases when the ER radius r increases. The relationship between $E[N]$ and the network density is shown in Fig. 5. It is observed that $E[N]$ increases rapidly with the increase of the total number of flows when r is small, and the difference disappears when r is large. When $r = 1 \text{ m}$, the average number of

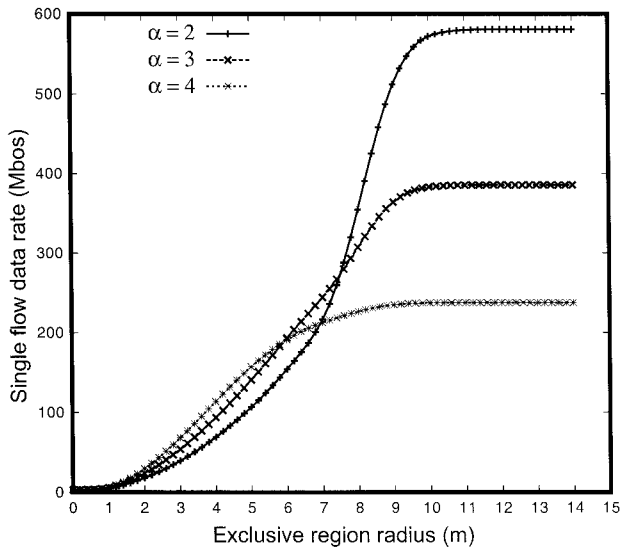


Fig. 6. Single flow data rate during transmission ($C_0 = 1$).

concurrent transmissions in the network increases from 9 to 46 when the total number of flows increases from 10 to 100. When $r = 2$ m, $E[N]$ increases from 6 to 17. When r is 6 m, only 2 to 3 flows can transmit concurrently no matter how many flows are in the network. Simulation results validate the accuracy of our analysis.

B. Network Capacity and Transport Capacity

In this subsection, we evaluate network performance considering constant channel gain $S = 1$ and the impact of channel fast fading will be investigated in the following subsection.

Given different path loss exponents, the relationship of the ER radius r and the data rate of a single flow during transmission is shown in Fig. 6. Basically, the average data rate of a flow is proportional to its average received SINR, which increases when the ER radius r becomes larger and the number of concurrent transmissions decreases. When r is small, more flows can transmit concurrently, which results in higher interference level that degrades the data rate of each flow significantly. When r is sufficiently large to forbid any concurrent transmission, only one flow transmits at a time in a serial TDMA transmission fashion and the maximum data rate of a single flow can be achieved with no interference. Notice that both signal and interference power levels are dependent on the path loss exponent α . When the ER radius r is small, interference is serious. A larger value of α may result in a drastic decrease of interference level and a higher SINR can be achieved. When r is large and there is no serious interference, the signal power decreases as α increases, so a lower data rate is achieved when α is larger. As shown in Fig. 6, when $r = 3$ m, flow data rate for $\alpha = 4$ is slightly larger than that for $\alpha = 3$ and $\alpha = 2$, in which cases, interference is the dominant factor of the single flow data rate. When $r \geq 9$ m, the data rate for $\alpha = 4$ is much less than that for $\alpha = 3$ and $\alpha = 2$, because in these cases the signal strength becomes the dominant factor.

The network capacity under various path loss exponents is shown in Fig. 7. It is observed that the network capacity in-

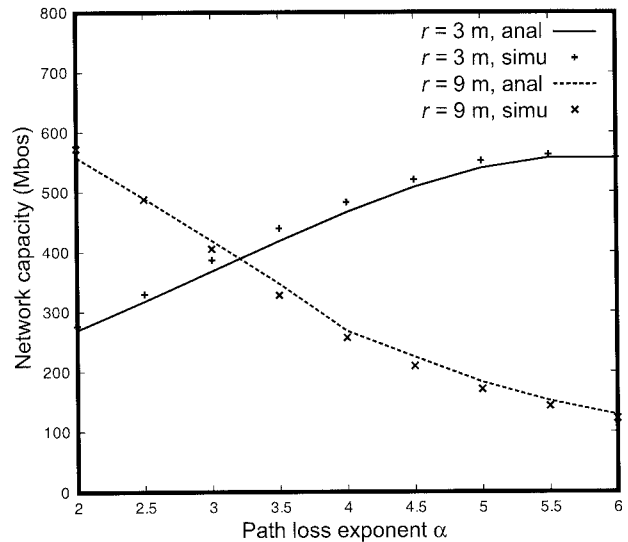


Fig. 7. Network capacity vs. path loss exponent α .

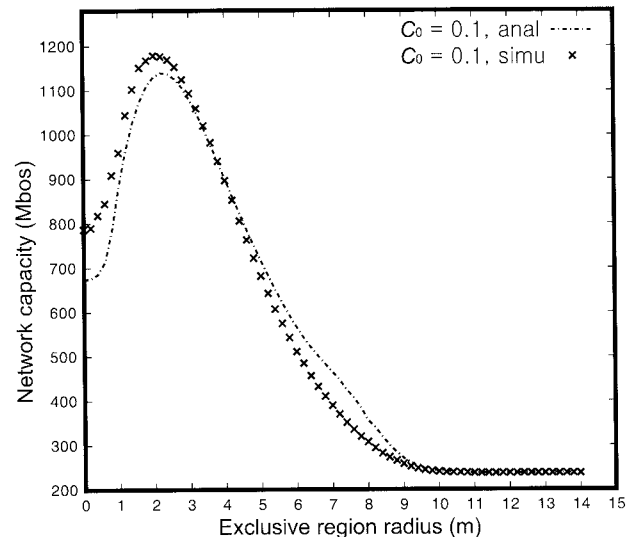
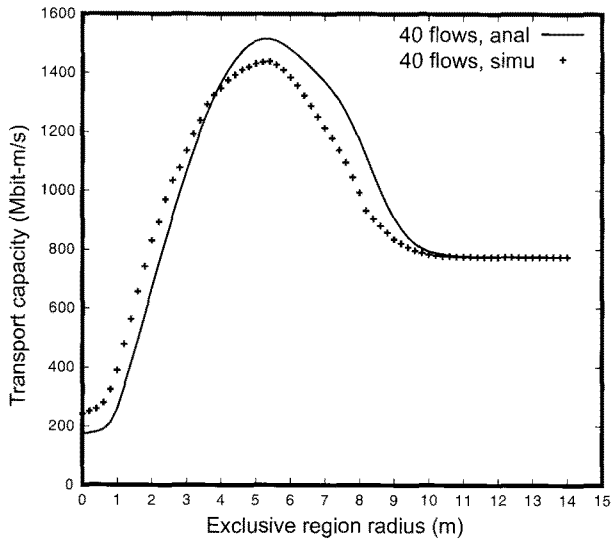
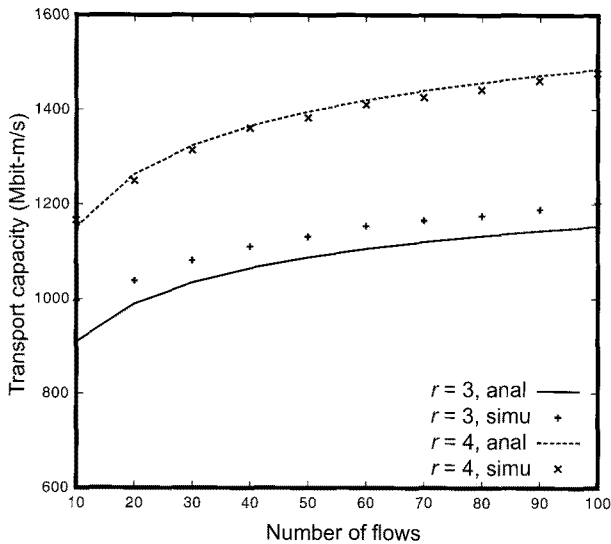


Fig. 8. Network capacity vs. ER radius ($\alpha = 4$).

creases with α when $r = 3$ m, but decreases when $r = 9$ m. Although the single flow data rate of $r = 3$ m is always smaller than that of $r = 9$ m, the total throughput when $r = 3$ m may be larger when the path loss is severe enough to significantly reduce the interference level. For $r = 9$ m, there is little spatial multiplexing gain since only one flow transmits at a time, as shown in Fig. 4; the network throughput equals that of a single flow throughput which decreases with α due to signal dispersion over distance.

We further investigate how the ER radius r affects the network capacity. As shown in Fig. 8, the network capacity is bounded by high interference level when r is small; and the capacity becomes constant and equals the average throughput of a single flow with a TDMA scheme when r is large enough to forbid any concurrent transmissions. Thus, the network capacity is a concave curve as a function of r . The maximum network capacity is achieved when r is around 4 m. The figures also show that the analytical results match well with the simulation ones.

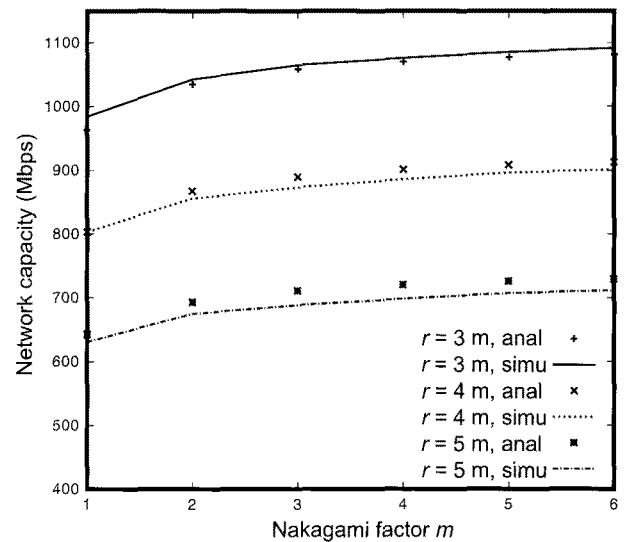
The transport capacity of the network is shown in Fig. 9.

Fig. 9. Transport capacity vs. ER radius ($\alpha = 4$).Fig. 10. Transport capacity vs. number of flows ($\alpha = 4$).

There are 40 flows in the network. The path loss exponent is 4 and $C_0 = 1$. Similar to the network capacity, the transport capacity of the network is also a concave curve under different ER radii and the maximum transport capacity is achieved when $r = 5$ m. The relationship between the transport capacity and network density under different ERs is investigated in Fig. 10. When the network is sparse, the transport capacity is relatively low because spatial reuse is not fully deployed. We increase the number of flows in the network, and the transport capacity improves with more flows transmitting concurrently. Given the ER size r , the expected number of concurrent transmissions will not increase rapidly with the total number of flows in a dense network, as shown in Fig. 5, and the increment of the transport capacity slows down accordingly.

C. Nakagami Fading

We then study the impacts of the Nakagami channel fading on network capacity. The network capacity under various Nak-

Fig. 11. Impacts of Nakagami channel fading ($C_0 = 0.1$).

agami fading parameter m ($m = 1 \sim 6$) is shown in Fig. 11. The parameter m generally reflects the severity of the channel fading conditions. The larger the m is, the more likely there is a line-of-sight path, and thus the better channel condition we have. It is observed that the network capacity increases as m increases.

VI. CONCLUSIONS

In this paper, we have developed an analytical framework to study the network capacity and transport capacity of UWB-based wireless networks in a 3D space, considering the characteristics of rate-adaptive wireless communication technologies. The analysis can help to determine the optimal ER size to maximize the network capacity by allowing appropriate concurrent transmissions. Due to the limited transmission distance of UWB communications, multiple piconets or multi-hop transmissions are necessary to extend the communication coverage. Further research is needed to investigate how to derive optimal ER size for multiple piconets cases or multi-hop UWB networks, considering the use of different types of antennae.

APPENDIX

A. PROBABILITY DENSITY FUNCTION OF DISTANCE IN 3D SPACE

To measure the signal and interference levels for network capacity study, the pdf of the distance among devices is required. In a 3D space, the distance distribution between two devices can be derived given the distributions of their coordinators in three dimensions. The following is an example of how to obtain the pdf of the distance for devices randomly deployed in an $l \times l \times h$ space, i.e., the three coordinators of each device are random variables with uniform distribution.

The probability distribution of the distances between two devices randomly (uniformly) located on a one-dimensional line or in a two-dimensional plane are known [20]. Based on the pdf of the distance on a unit line and in a unit square, we derive the cumulative distribution function (CDF) of the distance in 3D

space and obtain its pdf as follows.

Let X be the distance between two devices in an $l \times l$ square with uniform distribution. The pdf of X , $f_X(x)$, is a piecewise function given by

$$f_X(x) = \begin{cases} 2\frac{x}{l^2}(\frac{x^2}{l^2} - 4\frac{x}{l} + \pi) & \text{for } 0 \leq x \leq l \\ 2\frac{x}{l^2}(4\sqrt{\frac{x^2}{l^2} - 1} - (\frac{x^2}{l^2} + 2 - \pi)) & \\ -4 \tan^{-1} \sqrt{\frac{x^2}{l^2} - 1} & \text{for } l < x \leq \sqrt{2}l. \end{cases} \quad (\text{A-1})$$

Let Y be the distance between two devices randomly located on a line of length h . The pdf of Y , $f_Y(y)$, is given by

$$f_Y(y) = \frac{2}{h}(1 - \frac{y}{h}) \quad \text{for } 0 \leq y \leq h. \quad (\text{A-2})$$

Let Z be the distance between two devices randomly located in an $l \times l \times h$ space. The CDF of Z is derived as

$$\begin{aligned} \Pr(Z \leq z) &= \int_0^h \Pr(X \leq x | Y = y) f_Y(y) dy \\ &= \begin{cases} \int_0^h F_X(\sqrt{z^2 - y^2}) f_Y(y) dy & \text{for } z > h \\ \int_0^z F_X(\sqrt{z^2 - y^2}) f_Y(y) dy & \text{for } z \leq h \end{cases} \end{aligned} \quad (\text{A-3})$$

where $F_X(\sqrt{z^2 - y^2})$ can be obtained from (A-1) as follows:

$$F_X(\sqrt{z^2 - y^2}) = \int_0^{\sqrt{z^2 - y^2}} f_X(x) dx.$$

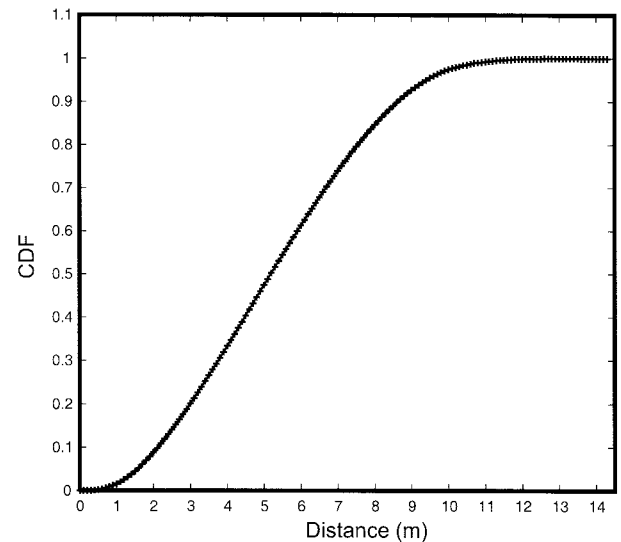
According to (A-1) and (A-3), $f_Z(z)$ is also a piecewise function. To simplify the presentation and analysis, we can use polynomial functions to fit the $f_Z(z)$ in each range:

$$f_Z(z) = \begin{cases} \sum_{i=1}^j a_{1i} z^i & \text{for } 0 \leq z \leq h \\ \sum_{i=1}^j a_{2i} z^i & \text{for } h < z \leq l \\ \sum_{i=1}^j a_{3i} z^i & \text{for } l < z \leq \sqrt{2l^2 + h^2} \end{cases} \quad (\text{A-4})$$

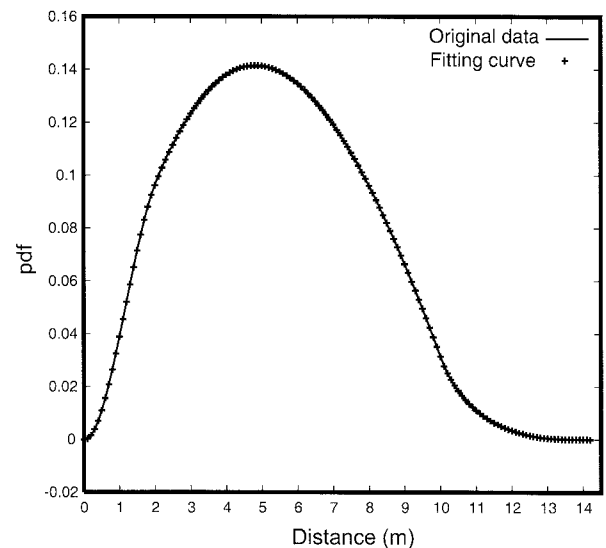
where j is the degree of the polynomials. For instance, using the polynomial fitting function in Matlab, we obtain the numerical results of the CDF and pdf of the distance between two devices randomly located in a room of $l = 10$ m and $h = 2$ m. The probability functions are shown in Fig. 12. The coefficient vectors of the three polynomials are

$$\begin{cases} \vec{a}_1 = [-0.016556, 0.058759, -0.00231682, -0.00012774], \\ \vec{a}_2 = [0.00019773, -0.007981, 0.063154, 0.0003309], \\ \vec{a}_3 = [-0.00053767, 0.022103, -0.30305, 1.3859]. \end{cases}$$

The errors introduced by the fitting functions of the third degree polynomials are less than 0.6%, as shown in Fig. 12.



(a)



(b)

Fig. 12. Distribution and probability functions ($l = 10$, $h = 2$): (a) CDF and (b) pdf.

REFERENCES

- [1] W. Zhuang, X. Shen, and Q. Bi, "Ultra-wideband wireless communications," *invited tutorial paper, Wireless Commun. and Mobile Comput. (WCMC)/Wiley - special issue on Ultra-Broadband Wireless Communications for the Future*, vol. 3, no. 6, pp. 663–685, 2003.
- [2] C. E. Shannon, "A mathematical theory of communication," *Bell Syst. Technical J.*, vol. 27, pp. 379–423, Jul. 1948.
- [3] X. Shen, W. Zhuang, H. Jiang, and J. Cai, "Medium access control in ultrawideband wireless networks," *IEEE Trans. Veh. Technol.*, vol. 54, no. 5, pp. 1663–1677, Sept. 2005.
- [4] R. Qiu, H. Liu, and X. Shen, "Ultra-wideband for multiple-access communications," *IEEE Commun. Mag.*, vol. 43, no. 2, pp. 80–87, 2005.
- [5] P. Gupta and P. Kumar, "The capacity of wireless networks," *IEEE Trans. Inf. Theory*, vol. 46, pp. 388–404, Mar. 2000.
- [6] P. Gupta and P. Kumar, "Internets in the sky: The capacity of three dimensional wireless networks," *Commun. Inf. Syst.*, vol. 1, pp. 39–49, 2001.
- [7] M. Grossglauser and D. N. C. Tse, "Mobility increases the capacity of ad-hoc wireless networks," in *Proc. IEEE INFOCOM*, 2001, pp. 1360–1369.
- [8] S. A. Jafar, "Too much mobility limits the capacity of wireless ad hoc networks," *IEEE Trans. Inf. Theory*, vol. 51, pp. 3954–3965, Nov. 2005.

- [9] M. Gastpar and M. Vetterli, "The capacity of wireless networks: The relay case," in *Proc. IEEE INFOCOM*, 2002.
- [10] H. Gamal, "On the scaling laws of dense wireless sensor networks: The data gathering channel," *IEEE Trans. Inf. Theory*, vol. 51, no. 3, pp. 1229–1234, 2003.
- [11] K. H. Alireza, R. Vinay, and R. Rudolf, "Broadcast capacity in multihop wireless networks," in *Proc. MobiCom*, 2006, pp. 239–250.
- [12] R. Zheng, "Information dissemination in power-constrained wireless networks," in *Proc. IEEE INFOCOM*, Apr. 2006, pp. 1–10.
- [13] R. Negi and A. Rajeswran, "Capacity of power constrained ad-hoc networks," in *Proc. IEEE INFOCOM*, vol. 1, pp. 443–453, Mar. 2004.
- [14] V. P. Mhatre and C. P. Rosenberg, "The impact of link layer model on the capacity of a random ad hoc network," in *Proc. IEEE ISIT*, Jul. 2006, pp. 1688–1692.
- [15] B. Radunovic and J. Le Boudec, "Optimal power control, scheduling, and routing in UWB networks," *IEEE J. Sel. Areas Commun.*, vol. 22, no. 7, pp. 1252–1270, Sept. 2004.
- [16] L. X. Cai, L. Cai, X. Shen, and J. W. Mark, "REX: A randomized exclusive region based scheduling scheme for mmWave WPANs with directional antenna," *IEEE Trans. Wireless Commun.*, to appear.
- [17] K.-H. Liu, L. Cai, and X. Shen, "Exclusive-region based scheduling algorithms for UWB WPAN," *IEEE Trans. Wireless Commun.*, vol. 7, no. 1, Jan. 2008.
- [18] L. X. Cai, L. Cai, X. Shen, and J. Mark, "Capacity of UWB networks supporting multimedia services," in *Proc. IEEE QShine*, Aug. 2006.
- [19] A. F. Molisch, "Ultrawideband propagation channels-theory, measurement, and modeling," *IEEE Trans. Veh. Technol.*, vol. 54, no. 5, pp. 1528–1545, Sept. 2005.
- [20] Math world, *Square Line Picking*. [Online]. Available: <http://mathworld.wolfram.com/SquareLinePicking.html>



Xuemin (Sherman) Shen received the B.Sc.(1982) degree from Dalian Maritime University (China) and the M.Sc. (1987) and Ph.D. degrees (1990) from Rutgers University, New Jersey (USA), all in electrical engineering. He is a Professor and University Research Chair in the Department of Electrical and Computer Engineering, University of Waterloo, Canada. His research focuses on mobility and resource management in interconnected wireless/wired networks, UWB wireless communications systems, wireless security, and ad hoc and sensor networks. He is a co-author of three books, and has published more than 300 papers and book chapters in wireless communications and networks, control and filtering. He serves as the Technical Program Committee Chair for IEEE Globecom'07, General Co-Chair for Chinacom'07 and QShine'06, the Founding Chair for IEEE Communications Society Technical Committee on P2P Communications and Networking. He also serves as a Founding Area Editor for *IEEE Transactions on Wireless Communications*; Associate Editor for *IEEE Transactions on Vehicular Technology*; *KICS/IEEE Journal of Communications and Networks*; *Computer Networks* (Elsevier); *ACM/Wireless Networks*; and *Wireless Communications and Mobile Computing* (John Wiley), etc. He has also served as Guest Editor for *IEEE JSAC*, *IEEE Wireless Communications*, and *IEEE Communications Magazine*. He received the Excellent Graduate Supervision Award in 2006, and the Outstanding Performance Award in 2004 from the University of Waterloo, the Premier's Research Excellence Award in 2003 from the Province of Ontario, Canada, and the Distinguished Performance Award in 2002 from the Faculty of Engineering, University of Waterloo. He is a registered Professional Engineer of Ontario, Canada.



Jon W. Mark received the Ph.D. degree in electrical engineering from McMaster University in 1970. In September 1970 he joined the Department of Electrical and Computer Engineering, University of Waterloo, Waterloo, Ontario, where he is currently a Distinguished Professor Emeritus. He served as the Department Chairman during the period July 1984–June 1990. In 1996 he established the Centre for Wireless Communications (CWC) at the University of Waterloo and is currently serving as its founding Director. He had been on sabbatical leave at the following places: IBM Thomas J. Watson Research Center, Yorktown Heights, NY, as a Visiting Research Scientist (1976-77); AT&T Bell Laboratories, Murray Hill, NJ, as a Resident Consultant (1982-83); Laboratoire MASI, Université Pierre et Marie Curie, Paris France, as an Invited Professor (1990-91); and Department of Electrical Engineering, National University of Singapore, as a Visiting Professor (1994-95). He has previously worked in the areas of adaptive equalization, image and video coding, spread spectrum communications, computer communication networks, ATM switch design and traffic management. His current research interests are in broadband wireless communications, resource and mobility management, and cross domain interworking. He is a co-author of the text *Wireless Communications and Networking*, Prentice-Hall 2003. A Life Fellow of IEEE and a Fellow of the Canadian Academy of Engineering, He is the recipient of the 2000 Canadian Award for Telecommunications Research and the 2000 Award of Merit of the Education Foundation of the Federation of Chinese Canadian Professionals. He was an editor of *IEEE Transactions on Communications* (1983-1990), a member of the Inter-Society Steering Committee of the *IEEE/ACM Transactions on Networking* (1992-2003), a member of the IEEE Communications Society Awards Committee (1995-1998), an editor of *Wireless Networks* (1993-2004), and an associate editor of *Telecommunication Systems* (1994-2004). He is currently a member of the Advisory Board of the J. Wiley Series on Advanced Texts in Communications and Networking.



Lin X. Cai received the B.Sc. degree in computer science from Nanjing University of Science and Technology, Nanjing, China, in 1996 and the M.A.Sc. degree in electrical and computer engineering from the University of Waterloo, Waterloo, Canada, in 2005. She is currently working toward a Ph.D. degree in the same field at the University of Waterloo. Her current research interests include network performance analysis and protocol design for multimedia applications over broadband wireless networks.



Lin Cai received the M.A.Sc. and Ph.D. degrees (with Outstanding Achievement in Graduate Studies Award) in electrical and computer engineering from the University of Waterloo, Waterloo, Canada, in 2002 and 2005, respectively. Since July 2005, she has been an Assistant Professor in the Department of Electrical and Computer Engineering at the University of Victoria, British Columbia, Canada. Her research interests span several areas in wireless communications and networking, with a focus on network protocol and architecture design supporting emerging multimedia traffic over wireless, mobile, ad hoc, and sensor networks. She serves as the Associate Editor for *IEEE Transactions on Vehicular Technology* (2007-), *EURASIP Journal on Wireless Communications and Networking* (2006-), and *International Journal of Sensor Networks* (2006-).